OPEN ACCESS

Applied Physics Express 14, 092004 (2021) LETTER

https://doi.org/10.35848/1882-0786/ac1a48

Characteristics of nonlinear terahertz-wave radiation generated by mid-infrared femtosecond pulse laser excitation

Kyuki Shibuya[1,2,3*], Kouji Nawata[3], Yoshiaki Nakajima[2,4], Yuxi Fu[5,6], Eiji J. Takahashi[5], Katsumi Midorikawa[5], Takeshi Yasui[2,7], and Hiroaki Minamide[3]

[1]Graduate School of Technology, Industrial and Social Sciences, Tokushima University, Japan
[2]JST, ERATO MINOSHIMA Intelligent Optical Synthesizer (IOS) Project, Japan
[3]Tera-Photonics Research Team, RIKEN Center for Advanced Photonics, RIKEN, Japan
[4]Department of Physics, Faculty of Sciences, Toho University, Japan
[5]Attosecond Science Research Team, RIKEN Center for Advanced Photonics, RIKEN, Japan
[6]Xi'an Institute of Optics and Precision Mechanics, Chinese Academy of Sciences, People's Republic of China
[7]Institute of Post-LED Photonics (pLED), Tokushima University, Japan

*E-mail: shibuya.tokudai@gmail.com

Received May 4, 2021; revised July 27, 2021; accepted August 3, 2021; published online August 18, 2021

We report on efficient terahertz-wave generation in organic and inorganic crystals by nonlinear wavelength conversion approach using a 3.3 μm femtosecond pulse laser. Experimental results reveal the relation between pump power and terahertz-wave output power, which is proportional to the square of the pump power at the range of mega- to tera-watt cm^{-2} class even if the pump wavelength is different. Damage threshold of organic and inorganic crystals are recorded 0.6 and 18 tera-watt cm^{-2} by reducing several undesirable nonlinear optical effects using mid-infrared source.

Supplementary material for this article is available online

Intense terahertz (THz) wave generation, based on the nonlinear wavelength conversion approach, has revealed various physical phenomena in the THz region, such as the Higgs mode in superconductors, nanoscale crystal growth, and shockwave generation.[1–3] Nonlinear crystals (NLCs),[4] gases,[5] and liquids[6] have been studied as potential sources for generating intense THz-wave radiation. THz-wave sources, which are based on nonlinear wavelength conversion, generally have high coherency and frequency tunability. Additionally, such THz-wave sources can easily achieve a high gain by considering the phase-matching condition. In particular, lithium niobate (LN) or organic NLCs are representative NLCs owing to their large second-order susceptibility, e.g., LN = 168 pm V^{-1} (d_{eff}),[7] 4-dimethylamino-N-methyl-4-stilbazolium tosylate (DAST) = 210–600 pm V^{-1} (d_{11}).[8,9] NLCs can effectively convert the wavelength by manifesting the phase-matching condition and using a near-infrared (NIR) pump source, whose wavelength corresponds to the low-absorption band in the NLCs. Therefore, an efficient conversion (more than 1%) can be achieved.[10] Further, the electric field strength and energy of the pulse can reach up to MV cm^{-1} and mJ order, respectively.[11]

Recently, one approach attracts researcher's attention, which uses longer pump wavelength for increasing an available photon density of pump light to excite the NLCs. It is attractive because it can avoid a saturation of the efficiency by multi-photon absorption (MPA), and it can reduce the damage of the NLCs. An efficient THz-wave generation using a mid-infrared (MIR) femtosecond (fs) laser by optical rectification (OR)[12] and generating an air-plasma[13] have been reported. In the prior study, only a DAST crystal was used.[12] For a higher conversion efficiency, researches with various experimental pumping conditions are indispensable. Up to now, the influence of stimulated Brillouin scattering, thermally damage and photo reflective effect have been explained. The exceptional advantage using a MIR pump source will be revealed by experimentally comparing it with several types of NLCs, because each NLCs have different optical characteristics.

The use of longer-wavelength light as a pump source could restrict undesirable nonlinear optical effects and generate a THz-wave with lower pump energy, according to Manley–Rowe relations.[14] Therefore, we can expect that the THz-wave output is proportional to the pump power even in longer wavelength pumping. However, despite the knowledge of wavelength conversion using a longer-wavelength excitation source, sufficient experimental studies have not been performed. Recently, a tera-watt (TW) class MIR fs laser has been developed by using the dual-chirped optical parametric amplification (DC-OPA) scheme.[15] The DC-OPA can control phase of electric field in an ultrafast pulse by adjusting a carrier envelope phase (CEP), and the use of CEP-controlled THz-wave is expected to open up new interactions between THz-wave and various matters. These high-intensity MIR sources are expected to efficiently generate THz-waves by reducing the MPA and absorption of second-harmonic generation (SHG) light. Additionally, MIR pumping is effective to reduce the self-focusing effect[16] which causes optical damage to NLCs, because the effect appears prominently at shorter wavelengths. Further, since the longer wavelength light has lower photon energy, it is expected to reduce the rise in temperature of the NLC when the light becomes the dominant absorption band. The DC-OPA laser has a low repetition frequency; therefore, it provides sufficient time for the NLCs to cool down.[17] In contrast, phase-matching condition in the MIR region is not as satisfying as in the NIR region. The absorption of the DAST and N-benzyl-2-methyl-4-nitroaniline (BNA) crystals in the MIR region is are very high,[18,19] and LN has high absorption.[20] Also, the phonon absorption in NLCs should

not be ignored. However, the advantages of the DC-OPA laser will overcome the indicated demerits for the efficient generation of THz-wave radiation.

In this letter, we report THz-wave generation using 3.3 μm and 1.5 μm fs pulse sources with inorganic/organic crystals; periodically-poled LN (PPLN), BNA, and DAST. By comparing the input/output characteristics in the case of NIR and MIR pumping, we reveal that the THz-output in MIR region obeys the second-order nonlinear process, even with large absorption. Additionally, high damage threshold of NLCs are confirmed by reducing undesirable nonlinear effects. We present a comprehensive study to show the characteristics of the THz-wave radiation generated with several types of NLCs and with MIR pumping source.

Figure 1 shows the schematic of the experimental setup of our 3.3 μm DC-OPA laser system,[15)] which consists of two amplification stages. The system delivers 21 mJ pulse energy with a pulse width of 70 fs and a repetition frequency of 10 Hz, the peak power was 300 GW, and its spectra is shown in Ref. 15. In comparison to the 3.3 μm experiment, we constructed an all-polarization-maintaining Er-doped fiber laser using a semiconductor saturable-absorber mirror (SESAM) for mode-locking.[21)] The output of the fiber laser was amplified to 150 mW by two stages of Er-doped fiber amplifiers (EDFA), the power was 8.4 kW. Table I lists the specifications of the pump sources.

We used the following NLCs at room temperature to generate the THz-waves: 5 mol% MgO-doped PPLN (period (Λ): 21 μm crystal^{-1} length (l_c): 5 mm, laboratory made, Λ: 68 μm/l_c: 2.7 mm, Λ: 89 μm/l_c: 2 mm, HC Photonics Corp.), DAST crystals (thickness [μm]: 100, 500, 900, 2100, 2540, laboratory-made), and BNA crystals (thickness [μm]: 100, 500, 870, 1330, 1890, laboratory-made). These laboratory-made crystals had no surface coatings and polishing. In the case of 3.3 μm pumping, the generated THz-wave was detected using a pyroelectric detector (JASCO Corp.). In contrast, the THz-wave radiation with 1.5 μm pumping was detected by a Fermi-level managed barrier diode (FMB diode, NTT Electronics Corp.) owing to its lower noise-equivalent power than that of the pyroelectric detector. The temporal electric fields were also measured by a time-domain spectroscopic (TDS) system with the NLCs functioning as emitter and a low-temperature-grown gallium arsenide (LT-GaAs) photoconductive antenna (PCA, G10620-11, Hamamatsu Photonics K. K) was employed as the receiver. For comparing the output value between different types of detectors, we have calibrated the value using the responsivity of the pyroelectric detector and the FMB diode. The value of the antenna and the FMB diode have been calibrated by using a same crystal and a pump condition. Also, in the experimental setup, we used a THz lens for focusing the THz-waves to the detector and several black-polyethylene sheets for filtering the pump light. Therefore, the bellow optical losses existed; Fresnel reflection loss caused by a crystal (incident plane; 13% of the 3.3 μm light, output plane; 15% of the THz-wave), insertion loss caused by the THz-lens (15%), and the absorption loss caused by black-polyethylene sheets (40%). Total loss was over 80%. The actual output power and the efficiency of the generated THz-wave were estimated to be several times higher than the presented values.

Figure 2 shows the input/output characteristics of the measured THz-waves pumped at 1.5 μm and 3.3 μm. Considering the phase-matching length and group-velocity dispersion at 3.3 μm pumping, we used 500 μm thick DAST and BNA crystals for generating the THz-waves. The range of pump peak power, which was controlled by a variable aperture, was 90 to 613 GW cm^{-2}, and maximum THz-wave output of DAST and BNA were 23 and 1 MW cm^{-2}, respectively. In the case of the PPLN (Λ: 68 μm, phase-matching frequency (f_{pm}) (backward): 0.61 THz[22)]), the pump peak power reached 18 TW cm^{-2}, and the maximum THz-wave output reached 664 MW cm^{-2}. The actual gain as THz-wave output per crystal length which was 0.64 MW mm^{-1} (45 nJ mm^{-1}). Also, in the case of 1.5 μm pumping, PPLN (Λ: 89 μm, f_{pm} (forward): 1.18 THz) was used in Fig. 2 and S1 (available online at stacks.iop.org/APEX/14/092004/mmedia), and THz-wave spectra and phase matching conditions are shown in Figs. S1 and S2.

The result revealed that the output power was proportional to the square of the pump power, even in different pump

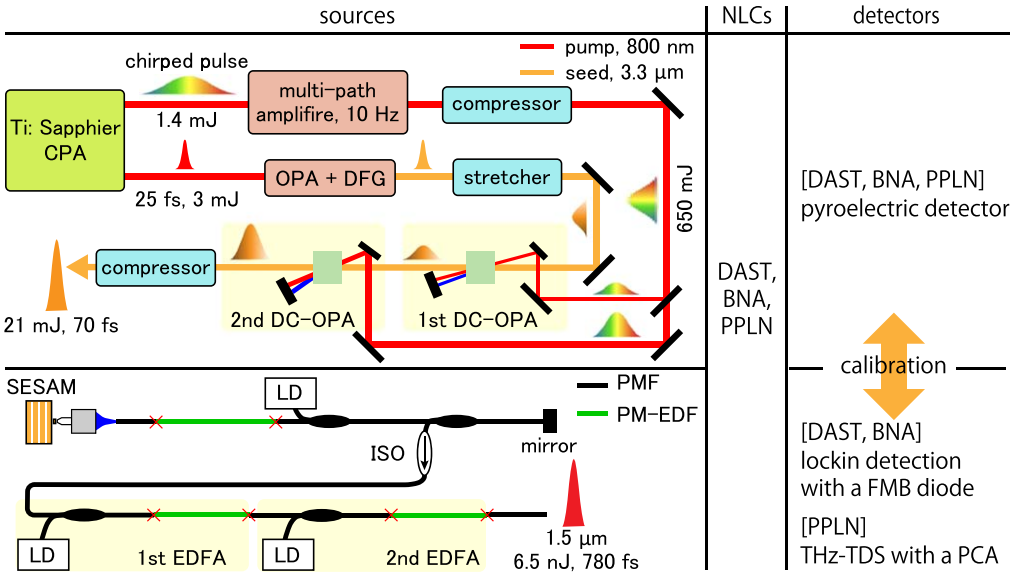

Fig. 1. (Color online) Illustration of the experimental setup.

Table I. Specifications of the pump sources.

	Center wavelength [μm]	Frep. [Hz]	Pulse energy [J]	Pulse width [fs]
DC-OPA laser	3.3	10	21×10^{-3}	70
Er-fiber laser	1.56	22.9×10^{6}	6.5×10^{-9}	780

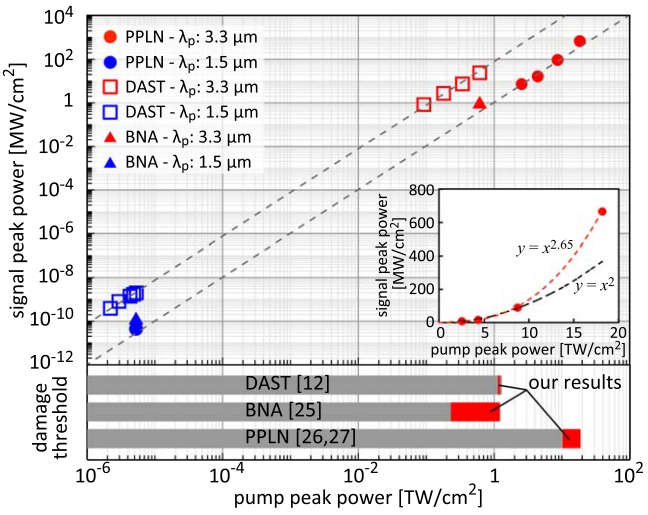

Fig. 2. (Color online) Comparison of the THz-wave output with pumping at 3.3 μm and 1.5 μm. The gray dotted line show square curve, and an inset shows the details of PPLN with 3.3 μm pumping. λ_p: pump wavelength.

wavelength and in very different pump power range. These seam-less relations can be understood from the theory of OR and the difference frequency generation. The relation includes contributions from the phase-matching condition and the absorption which is derived from the phonon-polariton mode.[23] And the absorption would be dominant when the phase-matching condition is almost not fulfilled. Also, the second-order nonlinear optical coefficient is almost constant from the NIR to MIR region.[24] This seam-less behavior includes the above several factors. In the MIR region, it is very interesting to confirm the output of THz-wave despite of the existence of large absorption. The behavior is explained due to the thickness of NLCs and its coherence length in shown Fig. 4. Moreover, the values of damage threshold of NLCs surpassed the previous reports,[25–27] as depicted at the bottom of Fig. 2. In the case of DAST, this behavior was reasonable while using the 3.3 μm DC-OPA because the repetition rate of less than 50 Hz and ultra-short pulses result in a high damage threshold owing to the reduced thermal effect.[17] The value was slightly lower than the previous report, because the absorption of DAST at 3.3 μm region was several times higher than 3.9 μm region. Further, saturation of the THz-wave output was not observed in this experiment and no optical damage occurred on both the NLCs.

It should be noted that the gradient of the output curve became larger thus the output itself showed a slight increase for the pumping PPLN at 18 TW, as depicted in the inset of Fig. 2; this was probably due to some cascade process. Hauri et al. reported the occurrence of a cascade process in DAST crystals.[10] However, we did not observe such a divergence.

For generating intense THz-waves, it is critical to consider the crystal composition and pumping conditions. In the case of PPLN, the LN crystal is damaged by an increased infrared absorption due to SHG.[28] The damage threshold of LN depends on the pulse width, wavelength of the pump source, and amount of MgO doping. Additionally, the thermal damage will increase if the pulse width is large.[26] Therefore, in fs pulse pumping, the damage threshold of the LN crystal without MgO doping is reported to be 10 TW cm^{-2}.[27] However, we confirmed that the THz-wave output increases when the pump power is increased to 18 TW cm^{-2}. The main reason for this increase was the difference in damage threshold for each pump wavelength,[26] and using MgO-doping LN crystal.[29]

Figure 3 shows a THz-wave output dependency of the pulse width at 3.3 μm pumping. The period of PPLN was 21 μm, and f_{pm} is 1.95 THz (backward). Here, the pump peak power was fixed at 5.1 TW cm^{-2}, and the pulse width was increased by adding several sapphire and CaF_2 crystals of different thicknesses. These efficiencies were normalized with peak pump power, then the energy conversion efficiency (η) was 1.8×10^{-4}. It is estimated that the efficiency was actually near 1% by considering the optical losses as already described. As a result, we revealed the optimum pulse width for efficient THz-wave generation.[30] Using a short pulse for pump light is an excellent method, however, as Nawata et al. demonstrated, the backward parametric oscillation in the THz region (Bw-TPO) using sub-nanosecond pulse could achieve high-power THz-wave generation.[31] In our experiment, the oscillation was not observed, although the pump peak power was higher than 1.6 GW cm^{-2}, which is the threshold of the Bw-TPO. The reason for the absence of the oscillations might be the low temporal interaction between pump light and generated THz-wave in the counter-propagating waves, which is caused by the fs pulse width.

In an NLC without a structure of periodically-pole, the thickness of the NLC is an important parameter because it affects nonlinear wavelength conversion efficiency.[10,32] Figure 4 shows the conversion efficiency of the DAST crystal. Figure 4(a) shows the case of 3.3 μm pumping. The pumping power was 600 GW cm^{-2}. We observed a decrease in the conversion efficiency when a crystal of thickness greater than 500 μm was used. Figure 4(b) shows the conversion efficiency at 1.5 μm pumping. The pumping power was 7 MW cm^{-2}. The conversion efficiency increased proportionally with the crystal thickness. These results are

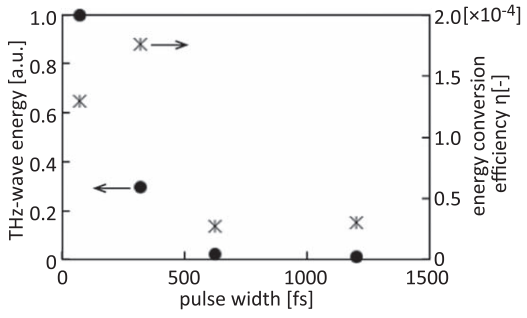

Fig. 3. The THz-wave energy and the efficiency in the 3.3 μm pumping PPLN.

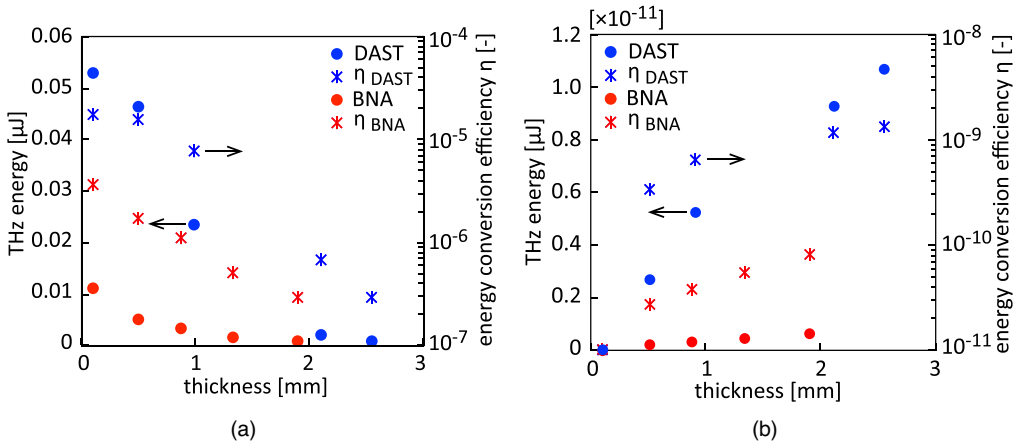

Fig. 4. (Color online) Relationship between the thickness of organic nonlinear crystals and THz-wave output. (a) 3.3 μm DC-OPA pumping. (b) 1.5 μm Er-doped fiber laser pumping.

explained by the coherence length and the absorption on NLCs. In the case of 3.3 μm pumping, the length of DAST crystal is 710 μm, the use of thicker crystal causes phase-mismatching owing to the absence of optical amplification in a crystal. In particular, high-frequency THz-wave might be limited by lack of coherence length when using thick crystals. In addition, an optical loss by the large absorption becomes dominant than the optical gain. As a result, the output and the efficiency decrease. Therefore, there is a possibility of higher THz-wave output by using thin crystals, which are less than 100 μm thickness and with large area size. In contrast, in the case of 1.5 μm pumping, the length is 140 μm. However, the output increased when the thicker crystal was used, because THz-wave was limited to a low-frequency region by using the pump light with narrow-bandwidth. Additionally, the pump light and THz-wave had low absorption.

In conclusion, we generated THz-wave using a TW class MIR ultra-short pulse source for overcoming the pumping limitation of NLCs. The experiment demonstrated an improvement in the damage threshold value to 613 GW cm^{-2} in the case of organic NLCs and to 18 TW cm^{-2} for inorganic NLCs. We could successfully avoid undesirable nonlinear optical effects. In particular, THz-wave generation with the large absorption is very interesting, and a high potential of MIR pumping for higher efficient THz-wave generation is expected.

The outcomes of our study can be useful for generating intense THz-waves using the nonlinear wavelength conversion method. Intense THz-wave generation using organic NLCs will be an attractive option because of their large second-order susceptibility, possibility of large area growth, printability, and flexibility. Furthermore, energy scaling would be a useful approach for increasing the THz-wave output without causing damage to the crystal. The total excitation energy can be improved by expanding the beam diameter and using a larger area of the NLCs while maintaining the energy density of the pump light. Based on energy scaling, we estimated that the output would be more than 6.7 and 0.2 GW (470 μJ and 15 μJ), if we use a 1 cm^2 PPLN and DAST crystal, respectively, without the optical component induced losses. These exceptional capabilities are useful for commercial and large-scale applications of THz-wave radiation.

Acknowledgments This study was supported by the Japan Society for the Promotion of Science (JP17H01282, JP18H01906); Exploratory Research for Advanced Technology (JPMJER1304). The authors thank all the members of the Tera-Photonics Laboratory at RIKEN for their helpful cooperation.

ORCID iDs Kyuki Shibuya https://orcid.org/0000-0001-6069-4057 Takeshi Yasui https://orcid.org/0000-0001-7742-6155

1) R. Matsunaga, Y. I. Hamada, K. Makise, Y. Uzawa, H. Terai, Z. Wang, and R. Shimano, Phys. Rev. Lett. **111**, 057002 (2013).
2) Y. Sanari et al., Phys. Rev. Lett. **121**, 165702 (2018).
3) J. Bühler, J. Allerbeck, G. Fitzky, D. Brida, and A. Leitenstorfer, Optica **5**, 821 (2018).
4) X.-C. Zhang, X. F. Ma, Y. Jin, and T.-M. Lu, Appl. Phys. Lett. **61**, 3080 (1992).
5) A. D. Koulouklidis, C. Gollner, V. Shumakova, V. Y. Fedorov, A. Pugžlys, A. Baltuška, and S. Tzortzakis, Nat. Commun. **11**, 292 (2020).
6) I. Dey et al., Nat. Commun. **8**, 1184 (2017).
7) J. Hebling, A. G. Stepanov, G. Almási, B. Bartal, and J. Kuhl, Appl. Phys. B **78**, 593 (2004).
8) U. Meier, M. Bösch, C. Bosshard, F. Pan, and P. Günter, J. Appl. Phys. **83**, 3486 (1998).
9) B. L. Lawrence, Master's Thesis Massachusetts Institute of Technology (1992), [https://dspace.mit.edu/handle/1721.1/13221].
10) C. Vicario, M. Jazbinsek, A. V. Ovchinnikov, O. V. Chefonov, S. I. Ashitkov, M. B. Agranat, and C. P. Hauri, Opt. Express **23**, 4573 (2015).
11) B. Zhang et al., Laser Photonics Rev. **15**, 2000295 (2021).
12) C. Gollner, M. Shalaby, C. Brodeur, I. Astrauskas, R. Jutas, E. Constable, L. Bergen, A. Baltuška, and A. Pugžlys, APL Photon **6**, 046105 (2021).
13) A. D. Koulouklidis, C. Gollner, V. Shumakova, V. Y. Fedorov, A. Pugžlys, A. Baltuška, and S. Tzortzakis, Nat. Commun. **11**, 1 (2020).
14) J. M. Manley and H. E. Rowe, Proc. IRE **47**, 2115 (1959).
15) Y. Fu, B. Xue, K. Midorikawa, and E. J. Takahashi, Appl. Phys. Lett. **112**, 241105 (2018).
16) G. Fibich and A. L. Gaeta, Opt. Lett. **25**, 335 (2000).
17) T. Matsukawa, K. Nawata, T. Notake, F. Qi, H. Kawamata, and H. Minamide, Appl. Phys. Lett. **103**, 023302 (2013).
18) C. Vicario, B. Monoszlai, G. Arisholm, and C. P. Hauri, J. Opt. **17**, 094005 (2015).
19) R. Kalaivanan and K. Srinivasan, Opt. Laser Technol. **90**, 27 (2017).
20) M. Leidinger, S. Fieberg, N. Waasem, F. Kühnemann, K. Buse, and I. Breunig, Opt. Express **23**, 21690 (2015).
21) L. C. Sinclair, J.-D. Deschênes, L. Sonderhouse, W. C. Swann, I. H. Khader, E. Baumann, N. R. Newbury, and I. Coddington, Rev. Sci. Instrum. **86**, 081301 (2015).
22) N. E. Yu, K. S. Lee, D. K. Ko, C. Kang, S. Takekawa, and K. Kitamura, Opt. Commun. **284**, 1395 (2011).
23) H. J. Bakker, S. Hunsche, and H. Kurz, Phys. Rev. B **50**, 914 (1994).
24) M. Jazbinsek, L. Mutter, and P. Gunter, IEEE J. Sel. Top. Quantum Electron. **14**, 1298 (2008).
25) M. Shalaby, C. Vicario, K. Thirupugalmani, S. Brahadeeswaran, and C. P. Hauri, Opt. Lett. **41**, 1777 (2016).
26) Y. Furukawa, A. Yokotani, T. Sasaki, H. Yoshida, K. Yoshida, F. Nitanda, and M. Sato, J. Appl. Phys. **69**, 3372 (1991).

27) Q. Meng, B. Zhang, S. Zhong, and L. Zhu, Appl. Phys. A **122**, 582 (2016).
28) Y. Furukawa, K. Kitamura, A. Alexandrovski, R. K. Route, M. M. Fejer, and G. Foulon, Appl. Phys. Lett. **78**, 1970 (2001).
29) Y. Kong, S. Liu, Y. Zhao, H. Liu, S. Chen, and J. Xu, Appl. Phys. Lett. **91**, 081908 (2007).
30) S. Carbajo, J. Schulte, X. Wu, K. Ravi, D. N. Schimpf, and F. X. Kärtner, Opt. Lett. **40**, 5762 (2015).
31) K. Nawata, Y. Tokizane, Y. Takida, and H. Minamide, Sci. Rep. **9**, 726 (2019).
32) H. Minamide and H. Ito, C. R. Phys. **11**, 457 (2010).